Available online at www.sciencedirect.com
ScienceDirect
C. R. Mecanique 335 (2007) 394–400
COMPTES RENDUS MECANIQUE
http://france.elsevier.com/direct/CRAS2B/

Dynamic behavior of a homogenized composite under contact with friction loading

Guillaume Peillex [a,*], Laurent Baillet [b], Yves Berthier [a]

[a] *LaMCoS, INSA-Lyon, CNRS UMR5259, 69621 Villeurbanne, France*
[b] *LGIT, maison des géosciences, 38400 Saint-Martin-d'Hères, France*

Received 22 August 2006; accepted after revision 3 April 2007

Available online 7 June 2007

Presented by Évariste Sanchez-Palencia

Abstract

This work is devoted to the numerical study of a composite under dynamic contact with friction loading, known as tribological loading. A dynamic explicit finite element model is used and Lagrange multipliers allow determining the local forces due to contact and friction. The convergence of numerical contact with friction models, achieved by using a regularized Coulomb friction law, is presented first. This study also shows the equivalence between the results obtained with heterogeneous and homogeneous materials under dynamical tribological loading. The homogeneous models are built by calling on classical homogenization theory because the main wavelength of the loading is much higher than that of the heterogeneities and the contrast between elastic properties is low. ***To cite this article: G. Peillex et al., C. R. Mecanique 335 (2007).***

Résumé

Homogénéisation et sollicitations dynamiques tribologiques des composites. Ce travail est dédié à l'étude numérique d'un composite sous sollicitations dynamiques de contact frottant appelées sollicitations tribologiques dynamiques. Un modèle éléments finis en dynamique explicite est utilisé et l'usage de multiplicateurs de Lagrange permet la détermination des forces dues au contact avec frottement. Dans un premier temps l'utilisation d'une loi de Coulomb régularisée permet de valider la convergence des modèles numériques de contact frottant en dynamique. Cette étude montre aussi l'équivalence des résultats de dynamique du contact obtenus entre des modèles hétérogènes et homogènes. Le comportement de ces derniers est calculé par la théorie classique de l'homogénéisation sous réserve que les longueurs d'ondes des modes excités lors du chargement soient largement plus grandes que la taille des hétérogénéités et que le contraste des propriétés élastiques des matériaux constituant le composite ne soit pas trop élevé. ***Pour citer cet article : G. Peillex et al., C. R. Mecanique 335 (2007).***

Keywords: Friction; Homogenization; Non-linear dynamics; Contact; Finite elements; Tribology

Mots-clés : Frottement ; Homogéneisation ; Dynamique non-linéaire ; Contact ; Éléments finis ; Tribologie

* Corresponding author.
E-mail address: guillaume.peillex@insa-lyon.fr (G. Peillex).

1631-0721/$ – see front matter
doi:10.1016/j.crme.2007.04.002

1. Introduction

Composite behavior under tribological loading is a difficult problem because it is a dynamic, multi-physical and multi-scale problem. It is dynamic because vibrations can occur and multi-scale because of the particular structure of the material. It has three scales: microscopic, composed of fibers ($\phi_{\text{fibre}} = 8$ μm) and a matrix; mesoscopic (characteristic length: 100 μm) composed of vertical layers (heterogeneities) embedded in a global matrix; and macroscopic (characteristic length: 10 cm). The material is transversely isotropic at this last scale.

A model has been built that takes into account all the specificities of loading and the material, though from a purely mechanical point of view. The physicochemical and thermal aspects of the problem are not taken into account in this study. The model consists of a composite pin, modeled with finite elements, rubbing against a steel disk which is replaced by a rigid surface as the stiffness of the steel is much greater than the stiffness of the composite. This is described in the first part of the study, which also provides a brief presentation of the model and the numerical algorithm. The second part of the study is devoted to the comparison between the mesoscopic scale and the macroscopic scale of the material. In what follows mesoscopic scale stands for heterogeneous while homogeneous stands for macroscopic scale. The second part illustrates that the homogeneous model obtained with static loading accurately represents the behavior of the composite pin under dynamical tribological loading. Since the wavelengths of the eigenmodes excited by the loading are much higher than the size of the heterogeneities and the contrast of elastic properties of the composite's constituents is low, the classical homogenization process [1], is used.

2. Numerical model

2.1. The composite studied

Here we focus primarily on the mesoscopic scale. The model composite (shown in Fig. 1) consists of a collection of heterogeneities embedded in a matrix. The volume rate of heterogeneities is ten percent. The properties of the matrix and the heterogeneities are summarized in Table 1. The heterogeneities are vertical as this is a characteristic of the real composite. They are about a hundred microns in width with a height from 1.2 to 3.6 millimeters.

The aim of this Note is to define a homogeneous model that represents the real behavior of the composite. The homogeneous model takes into account the presence of heterogeneities by using homogenized properties.

2.2. Homogenization of the composite material's properties

In order to determine the homogenized properties of the composite material (Table 1), six identical volumes (8 mm × 28 mm) with six randomized morphologies (i.e. randomized distributions of heterogeneities), were modeled in two dimensions with the commercial code Abaqus. The morphologies were assumed to be under plane strains with static loading. The properties were determined by using the classical theory of homogenization. Two different types of boundary conditions (stress or strain homogeneous on the contour $\Gamma = \Gamma_1 \cup \Gamma_2 \cup \Gamma_3 \cup \Gamma_4$) (Fig. 2) were

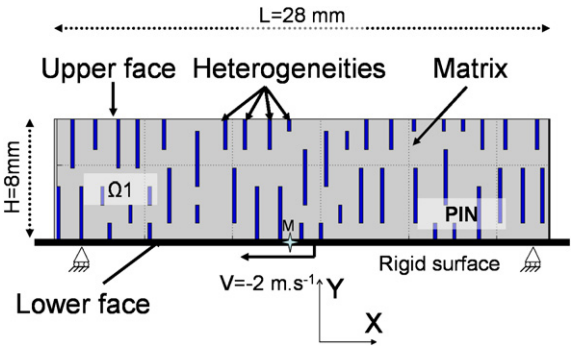

Fig. 1. Morphology of the model composite.

Fig. 1. Morphologie du composite modèle.

Table 1
Mechanical properties of the models. (L and T stand for longitudinal (along x) and transversal (along y), E stands for the Young modulus, ν for Poisson coefficient, G for shear modulus and ρ is the density)

Tableau 1
Propriétés mécaniques des modèles. (L et T signifient longitudinal (selon x) et transversal (selon y), E est le module de Young, ν est le coefficient de Poisson, G le module de cisaillement et ρ la densité)

Mesoscopical model		Homogeneous model
Heterogeneities	Matrix	Homogenized properties
$E = 80$ GPa	$E = 30$ GPa	$E_L = 31.9$ GPa $E_T = 34$ GPa
$\upsilon = 0.2$	$\upsilon = 0.2$	$\upsilon_{LT} = 0.2$ $\upsilon_L = 0.2$
$G = E/2(1+\upsilon)$	$G = E/2(1+\upsilon)$	$G_{LT} = 13.3$ GPa
$\rho = 1770$ kg/m^3	$\rho = 1770$ kg/m^3	$\rho = 1770$ kg/m^3

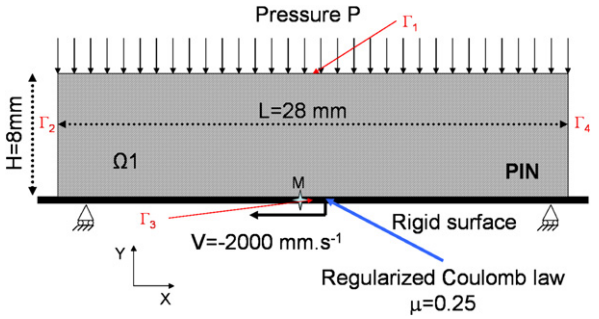

Fig. 2. Boundary conditions applied on a deformable/rigid contact model.

Fig. 2. Conditions aux limites appliquées sur un contact déformable/rigide.

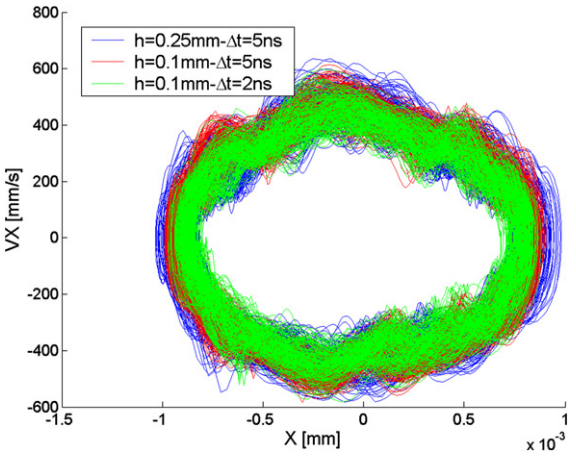

Fig. 3. Phase diagram of the central point in contact M for 2 different meshes ($h = 0.25$ mm coarse mesh, $h = 0.1$ mm fine mesh) and for 2 different time steps ($\Delta t = 5$ ns and $\Delta t = 2$ ns). Convergence through grid size and time step reduction by using regularized Coulomb friction law. ($\mu = 0.25$, $P = 0.5$ MPa, $V = -2\ \mathrm{m\,s^{-1}}$, $\beta = 1.1e^{-09}$, $\frac{L^*}{V} = 1500$ ns).

Fig. 3. Diagramme de phase du point central au contact M pour deux tailles de maille differentes et pour deux pas de temps differents. Convergence en maillage et en temps par utilisation de la loi de Coulomb régularisée.

applied in order to determine the five constants defining the behavior of a transversely isotropic material [2]. It was shown [3] that the results given by these two types of boundary conditions limit the exact result. The very low standard deviation between the results obtained with the two types of boundary conditions proves that the properties shown in Table 1 are very close to the exact ones.

2.3. Numerical model

As the simulations had to take into account non linear dynamic effects, PlastD [4,5] 2D explicit dynamic finite element laboratory code was used. This software uses the forward Lagrange multiplier (1) method to determine the contact forces, λ_n, and a Newmark-β_2 time integration scheme (2). Moreover it takes into account large deformations.

The equation of the forward increment Lagrange multiplier method is constructed using equations of motion developed via the principle of a virtual work equation at time t_n ($t_n = n\Delta t$) and the displacement constraints acting on the surfaces in contact at time t_{n+1}

$$\begin{cases} M\ddot{u}_n + C\dot{u}_n + Ku_n + G_{n+1}^T\lambda_n = f_n^{\text{ext}} \\ G_{n+1}\{x_n + u_{n+1} - u_n\} \leqslant 0 \\ C = \beta K \end{cases} \tag{1}$$

where G_{n+1} is the global matrix of the constraint, u_n and u_{n+1} are the displacement vectors at time t_n and t_{n+1}, x_n and x_{n+1} are the position vectors respectively at time t_n and t_{n+1}. M, C and K are respectively the mass, damping and stiffness matrices. β is a damping coefficient. f_n^{ext} are the nodal vectors of external forces. The dot and double dot superscript stands for first and second partial derivative with respect to time. At any time step, the velocity $\dot{u}_n$ and acceleration $\ddot{u}_n$ vectors are related to displacements and time step Δt in accordance with the β_2 method ($\beta_2 \in [0.5; 1[$)

$$\begin{cases} \dot{u}_n = \dfrac{1}{1+2\beta_2}\left[\dot{u}_{n-1} + \Delta t(1-\beta_2)\ddot{u}_{n-1} + \dfrac{2\beta_2}{\Delta t}(u_{n+1} - u_n)\right] \\ \ddot{u}_n = \dfrac{2}{\Delta t^2}(u_{n+1} - u_n - \Delta t\dot{u}_n) \end{cases} \tag{2}$$

In order to achieve stability and convergence of the β_2 method the time increment Δt must conform to the Courant–Friedrichs–Lewy condition

$$\Delta t \leqslant \frac{l_{\text{mini}}}{c_{\max}} \tag{3}$$

l_{mini} is the minimal element length and $c_{\max}$ is the maximal speed wave of the material. The time step Δt is equal to 5 ns throughout this study. The deformable/rigid model used is shown in Fig. 2. It consists of a rectangular pin ($\Omega 1$), modeled with linear quadrilateral finite elements under plane strains assumption, rubbing against a rigid flat surface which has a translation speed of $-2\ \text{m s}^{-1}$. A pressure, P, is applied on the top of the pin. The status of a node on the contact surface was obtained by using a friction law (4). The loading due to dynamic contact with a constant friction coefficient was neither uniform over the whole model nor constant [6,5,7]. Contact instabilities, coexisting with the waves, could occur and propagate in the model and were observed experimentally [8]. A regularized friction law, also known as 'simplified Prakash–Clifton law', was used (4) [9] in order to avoid convergence problems that can occur when using a classical Coulomb law to model solids rubbing against one each other numerically [10,11]. This regularized friction law links the tangential contact stress τ to the normal contact stress σ by way of the coefficient of friction μ

$$\begin{cases} |\tau^*| < \mu|\sigma| & \Rightarrow \quad \text{stick: } [\dot{u}] = 0;\ \tau = \tau^* \\ |\tau^*| > \mu|\sigma| & \Rightarrow \quad \begin{cases} \text{slip: } \dot{\tau} = -|V|/L^*(\tau - \alpha\mu|\sigma|) \\ \exists \gamma \geqslant 0 \text{ s.t. } [\dot{u}] = -\gamma\tau \end{cases} \end{cases} \qquad \alpha = \begin{cases} 1, & \tau^* \geqslant 0 \\ -1, & \tau^* < 0 \end{cases} \tag{4}$$

Here $[\dot{u}]$ stands for the relative tangential speed between a node at the interface and the rigid surface. τ^* is the tangential contact stress calculated under the sticking assumption and V is the sliding speed of the surface. L^* is a length parameter and the dot superscript stands for partial derivative relative to time. Throughout this study the friction coefficient μ is equal to 0.25 at every point of the model in contact with the rigid flat surface, and the ratio $\frac{L^*}{V}$ is equal to 300 times the time step. Convergence through grid size and time step reduction was achieved by using this particular friction law and are shown in Fig. 3.

3. Comparison of two scales for modeling the tribological behavior of a composite

This section deals with a comparison between a homogeneous model, with the properties described in Table 1, and a mesoscopic one, defined by heterogeneities embedded in the matrix whose properties are those of the two first columns of Table 1. Chen et al. [12] showed that for homogenization problems with highly contrasting elastic properties between the heterogeneities and matrix, it is necessary to take into account wave dispersion due to multiple reflection of the waves at the interface between the different materials of the composite. In the case presented here the elastic contrast is low and the dispersion phenomena is negligible. Moreover, the wavelengths of the eigenmodes excited in the model are much higher than the size of heterogeneities. For example the main frequency, f, of the normal stress in the contact zone is about 160 kHz. With a longitudinal wave speed, c, of the matrix equal to 4200 m/s^1 it corresponds to a wavelength $\lambda = \frac{c}{f}$ of about 26.25 mm. This value is approximately 10 times greater than the size of the heterogeneities. Furthermore, structural damping and regularized friction law allow the minimization of the influence of high frequencies and so decrease the risk of high frequencies reflection on the heterogeneities. From a purely dynamical point of view the material can be seen to be homogeneous [9]. The aim of this section is to establish whether the same conclusion can be drown under tribological loading.

The homogenization process does not take into account the dynamical parameters of the model such as the damping coefficient. To estimate the influence of this parameter on the calculations, simulations of the behavior of a composite beam in free vibration were performed with laboratory software. It was established that the damping coefficient in the homogeneous model had to be equal to that used in the mesoscopical model, Fig. 4. Throughout this study the damping term β is equal to $1.1e^{-09}$.

The applied pressure P on the finite element model (Fig. 2) successively takes values 0.5 MPa, 2.5 MPa and 5 MPa. These three cases correspond, for a friction coefficient μ equal to 0.25 (the same throughout this study), to three types of instabilities occurring at the interface of contact. Under low pressure, an arbitrarily chosen contact node slides on the rigid surface or is separated from it. This instability is called the 'slip-separated' instability. In the medium pressure range the 'stick-slip-separated' instability appears [7]. Under high pressure, all the contact nodes slide on the surface. A homogeneous and six randomized mesoscopic models were tested under each of these loading conditions.

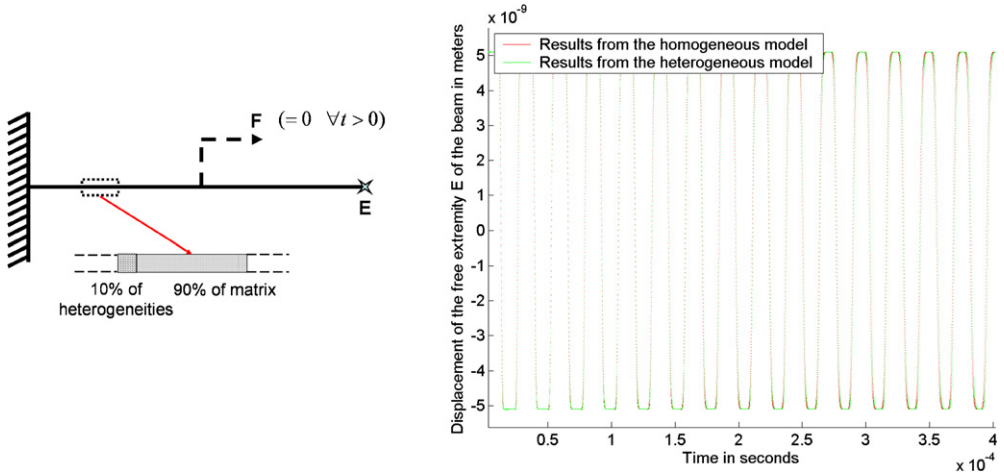

Fig. 4. Scheme and response of a composite beam and of the homogeneous equivalent beam subjected to free vibrations. The length of the beam is 28 mm and the volume fraction of heterogeneities is 10%. The elastic contrast is about $8/3$. The damping term β is equal to $1.1e^{-09}$ everywhere in the heterogeneous model and is the same in the homogeneous model.

Fig. 4. Schema et réponse d'une poutre composite et du modèle homogène équivalent en vibrations libres. La longueur de la poutre est de 28 mm et la fraction volumique d'hétérogénéités est de 10%. Le contraste élastique est de $8/3$. Le terme d'amortissement β est égal to $1.1e^{-09}$ partout dans le modèle hétérogène et est identique dans le modèle homogène.

The results presented below concern the global friction coefficient (Table 2) which is the ratio of the sum of the tangential forces (along x) at the upper face of the pin over the sum of the normal forces (along y) at the upper face of the pin. The phase diagram (Fig. 5), i.e. tangential speed of the point versus its tangential displacement, of the central point in contact, M (see Fig. 2) is also shown.

3.1. Low pressure; 'slip-separated' instabilities

In this section the applied pressure, P, has a value of 0.5 MPa which corresponds to a 'slip-separated' instability. The results presented in Fig. 5(a) are obtained with six different morphologies each of them having ten percent heterogeneity in volume. The six different morphologies give almost the same results, see Fig. 5(a). This means that, for the contrast of properties shown in Table 1, the volume chosen is representative of the composite. In Fig. 5(b) the results obtained with a homogeneous model with only matrix properties show that this model is not equivalent to the mesoscopic ones. However if the homogenized properties described in the last column of Table 1 are introduced in a homogeneous model then the results obtained are equivalent to those of the mesoscopic models. Consequently, an equivalent homogeneous model with a dynamic contact with friction loading was obtained, see Fig. 5(b).

3.2. Medium and high pressure; 'stick-slip-separated' and 'slip' instabilities

Others values of applied pressure, P, have been introduced in the model. A value of $P = 2.5$ MPa corresponds to a 'stick-slip-separated' instability and a value of $P = 5$ MPa corresponds to a 'slip' instability. For these loading cases two heterogeneous models have been compared to the homogeneous model. The results are not shown here but the model with homogenized properties gave a result very close to those given by the two mesoscopic models and for the two different types of instabilities occurring in the contact.

3.3. Conclusion

The work presented in this third part shows that, if the elastic contrast is low and if the wavelengths of the eigenmodes excited by the loading are much higher than the size of heterogeneities, the behavior of the homogeneous model, with homogenized properties obtained under static loading, is equivalent to that of the mesoscopic models,

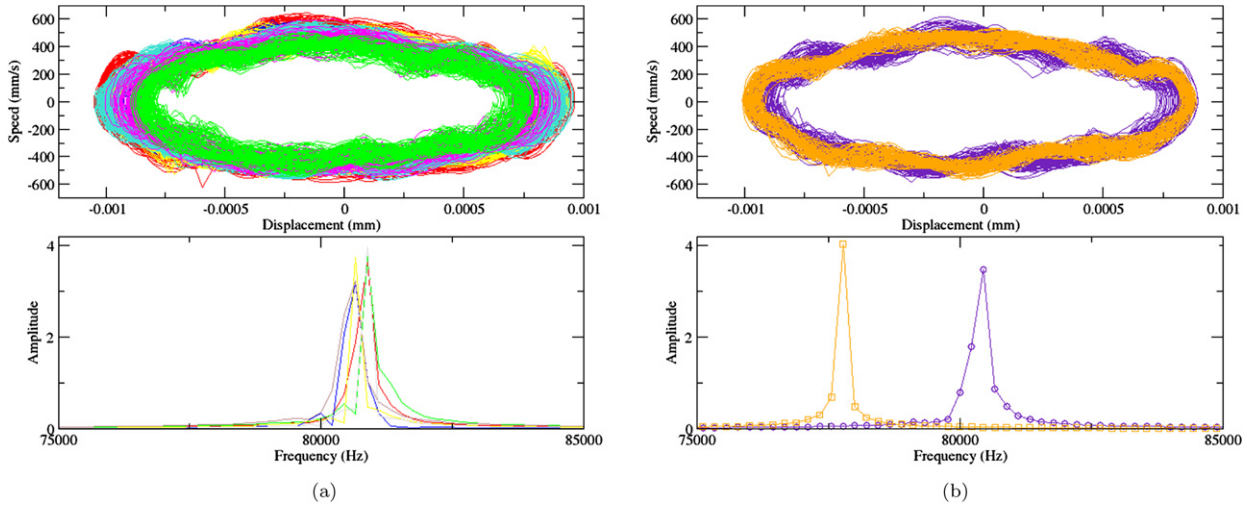

Fig. 5. $P = 0.5$ MPa; $\mu = 0.25$; 'slip-separated instabilities'. The top figure represents the phase diagram of the tangential movement of the central point in contact, M. The bottom figure represents the spectrum of the global friction coefficient. Left: results for six different morphologies with a volume rate of 10% of heterogeneities. Right: Results for two homogeneous models. Shaded: homogeneous with homogenized properties. Light: homogeneous with only matrix properties.

Fig. 5. $P = 0{,}5$ MPa ; $\mu = 0{,}25$; « instabilités de type glissement-décollement ». La figure du haut représente le diagramme de phase du mouvement tangentiel du point central au contact, M. La figure du bas représente le spectre du coefficient de frottement global. Gauche : Résultats pour six morphologies différentes ayant un taux volumique d'hétérogénéités de 10%. Droite : Résultats pour deux modèles homogènes. Foncé : homogène avec des propriétés homogénéisées. Clair : homogène avec seulement les propriétés de la matrice.

Table 2
The global friction coefficient averaged through time for different models and different loadings. The Homo. matrix model, which is the homogeneous model with only matrix properties (see Fig. 5(b)) gives results quite different from those of the mesoscopic models, whereas the model with homogenized properties gives results very close to those obtained with the mesoscopic models

Tableau 2
Le coefficient de frottement global moyenné au cours du temps pour différents modèles et différents chargements. Le modèle Homo. matrix, qui est le modèle homogène avec les propriétés de la matrice (cf. Fig. 5(b)) donne des résultats différents de ceux des modèles mésoscopiques, alors que le modèle homogène à propriétés homogénéisées donne des résultats proches de ceux obtenus avec les modèles mésoscopiques

Model	μ_{global} averaged		
	$P = 0.5$ MPa	$P = 2.5$ MPa	$P = 5$ MPa
Homo. matrix	0.183	0.234	0.245
Homo. homogenized	0.173	0.213	0.247
Mean of the meso.	0.176	0.210	0.246

whatever the type of instability occurring in the contact zone. This fact is confirmed by Table 2, which shows more quantitative results. The homogeneous model represents the macroscopic behavior of multiple mesoscopic models.

4. Conclusion

This numerical study demonstrated that a regularized Coulomb friction law allows good convergence of finite element models under dynamic contact with friction loading. A multiscale approach for composites under this particular loading is proposed and allows mapping two different scales. Thanks to a low contrast of elastic properties and a significant difference between the size of heterogeneities and the wavelength of the eigenmodes excited by the loading, mapping of the mesoscopic scale to the macroscopic one is performed by using the classical homogenization theory.

References

[1] E. Sanchez Palencia, Non-Homogeneous Media and Vibration Theory, Lecture Notes in Physics, vol. 127, 1980.

[2] J. Lemaitre, J.-L. Chaboche, Mécanique des matériaux solides, Dunod, 2004.
[3] M. Bornert, T. Bretheau, P. Gilormini, Homogénéisation en mécanique des matériaux, vol. 1, Matériaux aléatoires élastiques et milieux périodiques, Hermès Science, 2001.
[4] L. Baillet, T. Sassi, Finite element method with Lagrange multipliers for contact problems with friction, Comptes Rendus de l'Académie des Sciences I 334 (2002) 917–922.
[5] V. Linck, L. Baillet, Y. Berthier, Modeling the consequences of local kinematics of the first body on friction and on third body sources in wear, WEAR 255 (2003) 299–308.
[6] L. Baillet, V. Linck, S. D'Errico, B. Laulagnet, Y. Berthier, Finite element simulation of dynamic instabilities in frictional sliding contact, Journal of Tribology, Trans. ASME 127 (2005) 652–657.
[7] A. Oueslati, Q.-S. Nguyen, L. Baillet, Ondes adhérence-glissement-décollement sous contact unilatéral frottant: Stick-slip-separation waves in unilateral and frictional contact, Comptes Rendus de l'Académie des Sciences, Série IIB (February 2003) 133–140.
[8] G. Lykotrafitis, A.J. Rosakis, Sliding of frictionally held incoherent interfaces under dynamic shear loading, in: Proceedings of 2004 ASME/STLE International Joint Tribology Conference, 2004.
[9] G. Peillex, L. Baillet, Y. Berthier, Comparison between two scales for the modeling of composites under tribological solicitation, in: Proceedings of the ECCM 12, August 2006.
[10] K. Ranjith, J.R. Rice, Slip dynamics at an interface between dissimilar materials, Journal of the Mechanics and Physics of Solids 49 (2001) 341–361.
[11] A. Cochard, J.R. Rice, Fault rupture between dissimilar materials: Ill-posedness, regularization, and slip-pulse response, Journal of Geophysical Research 105 (2000) 25891–25907.
[12] W. Chen, J. Fish, A dispersive model for wave propagation in periodic heterogeneous media based on homogenization with multiple spatial and temporal scales, Journal of Applied Mechanics 68 (2) (2001) 153–161.